Coherently precessing states in ^{3}He-B

1993 J. Phys.: Condens. Matter 5 1759

(http://iopscience.iop.org/0953-8984/5/12/004)

J. Phys.: Condens. Matter 5 (1993) 1759–1768. Printed in the UK

Coherently precessing states in ^{3}He-B

G E Volovik
Landau Institute for Theoretical Physics, 117334 Moscow, Russia
and
Low Temperature Laboratory, Helsinki University of Technology, 02150, Espoo, Finland

Received 25 September 1992

Abstract. Several new stable states of coherent Larmor precession in superfluid ^{3}He-B have been found using both mean-field theory and numerical analysis.

Coherent Larmor precession of the magnetization in superfluid ^{3}He-B represents a time-dependent ordered state with the utmost broken symmetry in condensed matter. Such a precessing state has a rigidity that provides the high stability of coherent precession. This is the main feature of an ordered state with broken symmetry, and it distinguishes the dynamical ordered states in an essential way from the pattern-formation phenomena that take place in dissipative systems. Dissipation does not play an important part in these dynamical states of Larmor precession, since it is easily compensated by power supply from the applied radiofrequency field. The amplitude of the RF field is usually so small that it has no effect on the structure of the precessing state. The main role of the RF field is to choose such precessing states that are in resonance with the RF field. Therefore, the precessing states are described by broken symmetry principles and energy considerations, like the stationary states of condensed matter with broken symmetry.

One such anomalously stable coherent dynamical state, the homogeneously precessing domain (HPD), was discovered in 1984 as a result of both theoretical and experimental efforts [1], and is now used for the experimental investigation of topological objects in ^{3}He-B, such as axisymmetric and non-axisymmetric mass vortices [2] and combined spin–mass vortices with a soliton tail [3]. Until now only this HPD state has been exploited. However, there is evidence of other long-lived precessing states that are different from the conventional HPD [4]. On the other hand, numerical simulations [5] revealed long-lived regimes different to that discussed in [1]. Here we discuss several precessing states, which can be stabilized by shifting the frequency of the applied RF field from the Larmor value, by counterflow between the normal and superfluid motions, and by the magnitude of the applied RF field. These states can also be used for the investigation of ^{3}He-B, especially in the low-temperature limit when dissipation is small. Here we concentrate on the case when the magnitude of the magnetization is close to its equilibrium value: $|S| = \chi H$. Other states, which appear to be stable at special values of the spin magnitude, $|S| = \frac{1}{2}\chi H$ and $|S| = 2\chi H$, were found by Kharadze and Vachnadze [6] (see figure 1).

The Larmor precession of superfluid ^{3}He in the limiting case, when the spin–orbital (dipole) interaction is neglected, is highly degenerate and can be obtained by

0953-8984/93/121759+10$07.50

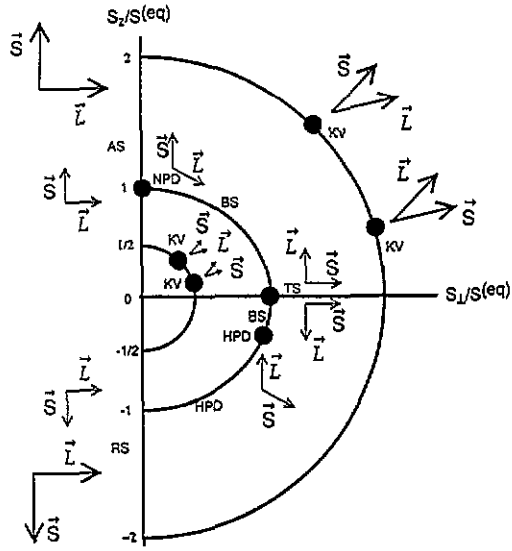

Figure 1. The homogeneously precessing states in the plane $S_z/S^{(eq)}$–$S_\perp/S^{(eq)}$, where $S^{(eq)} = \chi H_0$ is the equilibrium magnitude of the magnetization. The states discussed in this paper (figure 2) correspond to the equilibrium magnetization and occupy the half-circle of radius 1. The stable precessing states discovered by Kharadze and Vachandze [6] (KV states) have either double the value or half the value of the equilibrium magnetization. The equilibrium positions of the precessing states on the corresponding curves (full circles) depend on the frequency ω of the RF field; the points in the figure correspond to the case when ω approaches the Larmor frequency. HPD denotes the conventional homogeneously precessing domain (this name can be given to any of the discussed precessing states; historically this name was given to the branch of the BS state that continues below the point $S_z/S^{(eq)} = -1/4$). NPD denotes the stationary state. BS denotes the Brinkman–Smith mode. TS denotes the mode with transverse spin: this can be either the BS mode with $\hat{s}_z = 0$, $\hat{l}_z = 1$ or the mode with $\hat{s}_z = 0$, $\hat{l}_z = -1$, which is a bordering phase between the RS–TS mode and the RO mode (these two modes are not shown in figure 1; see figure 2). RS denotes states with reversed spin. AS denotes states with the spin aligned with the magnetic field.

two symmetry operations from the elementary initial stationary state; for example, with the equilibrium magnetization $S^{(0)} = \chi H$ [7]. These operations include orbital rotation in the laboratory frame and spin rotation in a frame rotating with the Larmor frequency $\omega_L = \gamma H$ (we further set the gyromagnetic ratio for the ^{3}He atom to be $\gamma = 1$). The latter symmetry results from the Larmor theorem, which states that the influence of a magnetic field on the spins of ^{3}He atoms completely disappears in a system rotating with the Larmor frequency. Therefore the spin rotation operation in the precessing frame does not change the Leggett equations for S and the order parameter. If $\mathbf{R}^{(S)}$ is the matrix of spin rotations in the precessing frame and $\mathbf{R}^{(L)}$ is the matrix of the orbital rotations in the laboratory frame, they define the orientation of the order-parameter matrix and magnetization $S_\alpha(t)$ for the general state of the Larmor precession.

For the isotropic B-phase state, where Cooper pairing occurs in the state with $J = 0$, the initial stationary state can be chosen with the following value of the 3×3 matrix order-parameter: $A^{(0)}_{\alpha i} = \text{constant} \times \delta_{\alpha i}$. Applying the symmetry operations to this

state one obtains the general precessing B-phase state $A(t)_{\alpha i} = \text{constant} \times R_{\alpha i}(t)$, where the time-dependent orthogonal matrix R is

$$\begin{aligned} R_{\alpha i}(t) &= O_{\alpha\beta}(\hat{z}, \omega_L t) R^{(S)}_{\beta\gamma} O_{\gamma\mu}(\hat{z}, -\omega_L t) R^{(L)}_{\mu i} \\ S_\alpha(t) &= O_{\alpha\beta}(\hat{z}, \omega_L t) R^{(S)}_{\beta\gamma} S^{(0)}_\gamma . \end{aligned} \tag{1}$$

Here $\mathbf{O}(\hat{z}, \omega_L t)$ describes the transformation from the laboratory frame into the rotating frame—this is a rotation about the z axis (along $\boldsymbol{H}$) by the angle $\omega_L t$. Equation (1) shows that the symmetry operation related to the spin subsystem contains (i) the transformation from the laboratory frame into the precessing frame, then (ii) the $\mathbf{R}^{(S)}$ rotation within this frame and after that (iii) the inverse transformation back to the laboratory frame.

The space of the degenerate states with Larmor precession is larger than for the stationary states. Though the dynamical state is described by one time-dependent orthogonal matrix $\mathbf{R}(t)$, which can be represented in terms of the axis $\hat{n}(t)$ and the angle $\theta(t)$ of rotation, each state is nevertheless characterized by two time-independent matrices, $\mathbf{R}^{(S)}$ and $\mathbf{R}^{(L)}$. This is distinct from the single time-independent degeneracy parameter $\mathbf{R} = \mathbf{R}^{(S)}\mathbf{R}^{(L)}$ that characterizes the stationary B-phase. The physical meaning of these two matrices is as follows. The $\mathbf{R}^{(S)}$ matrix shows the orientation of the spin in the precessing frame according to (1), $S^{\text{pr frame}}_\beta = R^{(S)}_{\beta\gamma} S^{(0)}_\gamma$. If $\hat{s} = \boldsymbol{S}^{\text{pr frame}}/|\boldsymbol{S}|$ is the direction of the magnetization in the precessing frame, then its projection on $\boldsymbol{H}$ is $\hat{s}_z = R^{(S)}_{zz}$. The $\mathbf{R}^{(L)}$ matrix shows the orientation $\hat{l}$ of the orbital momentum of Cooper pairs, which is defined as $L_i = -R_{\alpha i}(t) S_\alpha(t)$. From equation (1) it follows that $L_i = -R^{(L)}_{\alpha i} S^{(0)}_\alpha$ is constant in the laboratory frame. We choose here the opposite direction of the unit vector of the orbital momentum: $\hat{l} = -\boldsymbol{L}/|\boldsymbol{S}|$. If $\hat{l}_z$ is the z projection of $\hat{l}$, one has $\hat{l}_z = R^{(L)}_{zz}$.

Four terms contribute to the energy of the coherently precessing state and lift the degeneracy (the $S^2 \times SO(3)$ degeneracy, see [7]) of the general Larmor precession.

(i) The dipole energy (A4), after averaging over the period of precession, depends on only three degeneracy parameters, $\hat{s}_z$, $\hat{l}_z$ and Φ (this energy was first constructed by Fomin [8], who used a different set of degeneracy parameters):

$$\begin{aligned} F_D = \tfrac{2}{15}\chi\Omega_L^2 \{ &[\hat{s}_z \hat{l}_z - \tfrac{1}{2} + \tfrac{1}{2}\cos\Phi(1+\hat{s}_z)(1+\hat{l}_z)]^2 + \tfrac{1}{8}(1-\hat{s}_z)^2(1-\hat{l}_z)^2 \\ &+ (1-\hat{s}_z^2)(1-\hat{l}_z^2)(1+\cos\Phi)\}. \end{aligned} \tag{2}$$

Here Ω_L is the Leggett frequency, which we consider to be small, $\Omega_L^2/\omega_L^2 \ll 1$, and the variable Φ can be defined in the following way: if one introduces the Euler angles for the matrices $\mathbf{R}^{(L)}$ and $\mathbf{R}^{(S)}$, $\mathbf{R} = \mathbf{R}_z(\alpha)\mathbf{R}_y(\beta)\mathbf{R}_z(\gamma)$, then $\Phi = \alpha^{(S)} + \gamma^{(S)} - \alpha^{(L)} - \gamma^{(L)}$. Note the symmetry between the spin and orbital vectors $\hat{s}$ and $\hat{l}$ in the dipole energy.

(ii) The so-called spectroscopic term appears if the frequency, ω, of the RF field deviates from Larmor frequency, ω_L. In this case the Zeemann energy $-\boldsymbol{H}\cdot\boldsymbol{S}$ is not compensated completely by the Larmor energy of precession, $\boldsymbol{\omega}\cdot\boldsymbol{S}$; therefore one has a difference, which is the Zeeman energy in the frame, rotating with the frequency of the RF field [9]:

$$F_\omega = (\boldsymbol{\omega} - \boldsymbol{H})\cdot\boldsymbol{S} = \chi\omega_L(\omega - \omega_L)\hat{s}_z . \tag{3}$$

(iii) The interaction of the counterflow with the orbital anisotropy vector $\hat{l}$ (see, for example, [10]):

$$F_{\text{counterflow}} = -\tfrac{1}{2}\rho_a[(v_s - v_n)\cdot\hat{l}]^2 \tag{4}$$

where ρ_a is the anisotropy of the superfluid density, which is induced by the magnetic field.

(iv) The interaction of the magnetization with the transverse RF field:

$$F_{\text{RF}} = -\boldsymbol{H}_{\text{RF}}\cdot\boldsymbol{S}. \tag{5}$$

The equilibrium states are obtained by the minimization $F = F_{\text{counterflow}} + F_\omega + F_D + F_{\text{RF}}$:

$$\begin{aligned}\tilde{F} = u\hat{l}_z^2 + w\hat{s}_z + \{[\hat{s}_z\hat{l}_z - \tfrac{1}{2} + \tfrac{1}{2}\cos\Phi(1+\hat{s}_z)(1+\hat{l}_z)]^2 + \tfrac{1}{8}(1-\hat{s}_z)^2(1-\hat{l}_z)^2 \\ + (1-\hat{s}_z^2)(1-\hat{l}_z^2)(1+\cos\Phi)\} - h\sqrt{1-\hat{s}_z^2}\end{aligned} \tag{6}$$

where we normalized the energy in terms of the dipole energy, introducing the dimensionless variables

$$\begin{aligned}\tilde{F} &= \frac{15F}{2\chi\Omega_L^2} \qquad w = \frac{15\omega_L(\omega-\omega_L)}{2\Omega_L^2} \\ u &= \frac{15\rho_a(v_s-v_n)^2}{4\chi\Omega_L^2} \qquad h = \frac{15\omega H_{\text{RF}}}{2\Omega_L^2}\cos\alpha.\end{aligned} \tag{7}$$

In the last term α is the angle between the transverse magnetization and the transverse RF field; this term forces the magnetization to precess with the frequency ω of the RF field. The angle α is close to zero when the dissipation is small.

As distinct from [11], where the phase diagram in the w–u plane was constructed, we shall concentrate on the case when the counterflow is absent, $u = 0$, but instead consider the case of strong RF fields h, which can compete with other interactions and can thus stabilize some phases that are otherwise unstable. Minimization shows that there are at least six different stable or metastable states, which correspond to local energy minima (see figure 2).

(i) The non-precessing state (NPD). This is the stationary state with equilibrium magnetization, $\hat{s}_z = 1$, and with orbital angular momentum within the range $-\frac{1}{4} < \hat{l}_z < 1$. In this range the dipole energy is exactly zero..

(ii) The HPD mode. This mode has been extensively studied, both theoretically and experimentally (see [12]). It has $\cos\Phi = 1$, fixed orbital momentum $\hat{l}_z = 1$, and magnetization in the range $-1 < \hat{s}_z < -\frac{1}{4}$. The equilibrium value of magnetization within this range is defined by h and w. For small h:

$$\hat{s}_z = -\tfrac{1}{4} - \tfrac{1}{8}w.$$

This solution exists only for positive frequency shifts, $w > 0$.

(iii) The Brinkman–Smith (BS) mode. This is the mirror image of the NPD state: it has $\hat{l}_z = 1$, and spin within the range $-\frac{1}{4} < \hat{s}_z < 1$. The dipole energy is also exactly zero in this state. For $h \to 0$ this solution exists only at $w = 0$ and is unstable

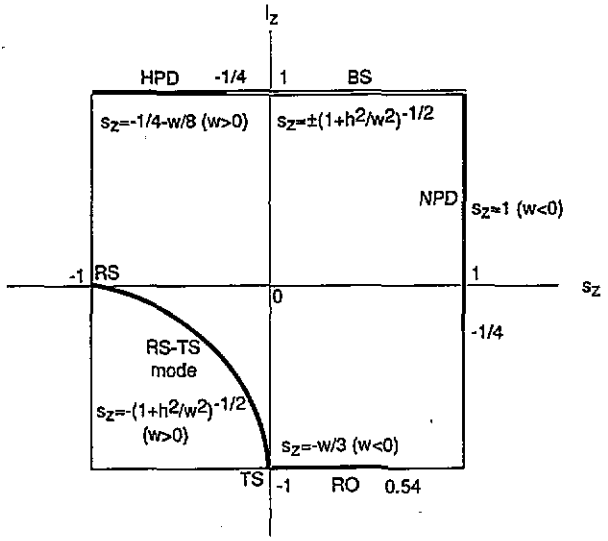

Figure 2. The homogeneously precessing states with an equilibrium magnitude of magnetization, $S = S^{(eq)}$, in the $\hat{l}_z$–$\hat{s}_z$ plane, where $\hat{s}_z = S_z/S$, $\hat{l}_z = -L_z/S$. In addition to the modes discussed in figure 1, RS–TS denotes states on the curve $(1-\hat{s}_z)(1-\hat{l}_z) = 2$ connecting the RS and TS points, and RO denotes the mode with the reversed orbital momentum. The equilibrium values of the longitudinal spin component $\hat{s}_z$ for the precessing states are shown in terms of the normalized frequency shift, w, and in terms of the normalized magnitude of the transverse RF field, h, if the latter is important for stability. For $w \to 0$ these equilibrium states are shown by full circles in figure 1.

towards HPD or NPD, or to HPD–NPD two-domain precession [12]. It is stabilized due to finite h and appears to exist for both positive and negative frequency shifts ω. This state is found from minimization of the spectroscopic and RF terms

$$w\hat{s}_z - h\sqrt{1-\hat{s}_z^2} \tag{8}$$

which gives the following equilibrium spin projection:

$$\hat{s}_z = -\frac{1}{\sqrt{1+h^2/w^2}}\operatorname{sign} w \tag{9}$$

where

$$h/w = \gamma H_{RF}/(\omega - \omega_L). \tag{10}$$

At zero frequency shift the equilibrium magnetization is perpendicular to the magnetic field: $\hat{s}_z = 0$.

(iv) The precessing state with reversed spin (RS). At small h the following solution exists: $\hat{s}_z = -1$, $\hat{l}_z = 0$, while Φ is arbitrary. This RS state differs by the orientation of $\hat{l}$ from another solution with $\hat{s}_z = -1$, which exists on the edge of the HPD line and is unstable according to Fomin [12]. This new RS state is degenerate on the two-dimensional surface: one degree of freedom comes from the arbitrary orientation of

$\boldsymbol{L}$ in the transverse plane and the other from Φ. From (1) it follows that the order parameter in the state with $\hat{l} = \hat{x}$ is given in terms of the axis $\hat{n}(t)$ and the rotation angle $\theta(t)$ of the dynamical matrix $\mathsf{R}(t)$ in the following way:

$$\cos\theta = -\cos^2\omega t \qquad \hat{n}\sin\theta = \hat{y}\sin^2\omega t + (\hat{z} - \hat{x})\sin\omega t\cos\omega t. \tag{11}$$

Let us consider the corrections to the average ('mean-field') description of the RS state. The dipole torque (A3)

$$\boldsymbol{T} = \tfrac{16}{15}\Omega_L^2\hat{n}\sin\theta(\cos\theta + \tfrac{1}{4}) \tag{12}$$

is non-zero in the RS state and thus leads to oscillations of the longitudinal spin component:

$$\delta S_z(t) = \int \mathrm{d}t\, T_z = \frac{1}{15}\frac{\Omega_L^2}{\omega^2}S(\cos 2\omega t + \tfrac{1}{2}\cos 4\omega t). \tag{13}$$

As a result the difference between the upper and lower values of the z projection of spin is

$$\Delta S_z = 0.15\frac{\Omega_L^2}{\omega^2}S. \tag{14}$$

This shows the range of applicability of the mean-field approximation in which such oscillations are neglected: $\Omega_L^2/\omega^2 \ll 1$.

It is important to note that it is difficult to maintain the RS state by the transverse RF field. Since the magnetization is nearly antiparallel to the constant field the transverse component of magnetization is rather small. Therefore the coupling with the pumping RF field practically disappears and nothing opposes the relaxation: (A5) cannot be satisfied. One way of relaxation for this state, which was observed in numerical analysis, is longitudinal relaxation: the spin is aligned antiparallel to the field, $\hat{s}_z = S_z/S = -1$, but the magnitude $|\boldsymbol{S}|$ of the magnetization decreases from the equilibrium value $|\boldsymbol{S}| = \chi H$. Finally, this state relaxes to the metastable Kharadze–Vachnadze (KV) state with $|\boldsymbol{S}| = \frac{1}{2}\chi H$. This provides the method for reaching KV states in NMR experiments.

(v) The RS–TS states. At $h \neq 0$ the RS mode appears to be a particular case of a whole family of states, situated between the RS mode and a mode with transverse spin (TS), which we call the RS–TS curve (figure 2). In these states

$$\cos\Phi = -1$$

which gives

$$\tilde{F}_D = \tfrac{3}{4} + \tfrac{3}{8}[(1 - \hat{s}_z)(1 - \hat{l}_z) - 2]^2. \tag{15}$$

The RS–TS mode corresponds to the minimum of (15)

$$(1 - \hat{s}_z)(1 - \hat{l}_z) = 2 \tag{16}$$

with the energy $\tilde{F} = 3/4$. As in the BS mode, for $h \to 0$ this solution exists only when $w = 0$, while at finite h it is stabilized by competition between the spectroscopic and

Table 1. The equilibrium values of the longitudinal component of magnetization $\hat{s}_z$ in RO ($\hat{s}_z > 0$) and RS–TS ($\hat{s}_z < 0$) states obtained by numerical analysis ($\hat{s}_z$ (num)) and in the mean-field theory ($\hat{s}_z$ (anal)).

ω/ω_L	H_{RF} (G)	Γ (kHz)	$\hat{s}_z$ (num)	w	h	$\hat{s}_z$ (anal)
0.994	2	30	+0.23	−0.81	0.4	+0.24
0.996	2	30	+0.14	−0.54	0.4	+0.16
0.997	2	30	+0.10	−0.40	0.4	+0.12
0.9975	2	30	+0.08	−0.34	0.4	+0.10
0.998	2	30	+0.04	−0.27	0.4	+0.08
0.999	2	30	−0.01	−0.13	0.4	+0.04
0.9995	2	30	−0.07	−0.07	0.4	+0.02
1.000	2	30	−0.15	0	0.4	0
1.0005	2	30	−0.25	+0.07	0.4	−0.16
1.001	2	30	−0.37	+0.13	0.4	−0.31
1.002	2	30	−0.57	+0.27	0.4	−0.55
1.003	2	30	−0.72	+0.40	0.4	−0.70
1.004	2	30	−0.82	+0.54	0.4	−0.80
1.0045	2	30	−0.84	+0.61	0.4	−0.83
1.005	2	30	−0.86	+0.68	0.4	−0.86
1.007	5	15	−0.68	+0.94	1.0	−0.68
1.010	5	15	−0.80	+1.35	1.0	−0.80
1.015	7	15	−0.82	+2.0	1.4	−0.82
1.015	6	15	−0.86	+2.0	1.2	−0.86
1.020	5	15	−0.93	+2.7	1.0	−0.93
1.025	5	15	−0.96	+3.4	1.0	−0.96

the RF terms, with the same equilibrium value of the longitudinal spin component (see (9)):

$$\hat{s}_z = -\frac{1}{\sqrt{1+h^2/w^2}}. \tag{17}$$

However, this state is stable only when $w > 0$. For $w < 0$ it can be stabilized only by the counterflow. In table 1 the mean-field result of equation (17), $\hat{s}_z$(anal), is compared with the exact results of numerical analysis, $\hat{s}_z$(num), obtained using a computer program developed by Leman and Golo [5].

(vi) The mode with reversed orbital momentum (RO). At $w < 0$, if there is no counterflow, the RS–TS mode is unstable towards the mode with reversed orbital momentum, $\hat{l}_z = -1$. This state is obtained by minimization of all three energy terms with $\cos\Phi = -1$

$$\tilde{F} = \tfrac{3}{4} + \tfrac{3}{8}[(1-\hat{s}_z)(1-\hat{l}_z) - 2]^2 + w\hat{s}_z - h\sqrt{1-\hat{s}_z^2}. \tag{18}$$

For small $\hat{s}_z$ or small h we obtain the following results for the equilibrium magnetization:

$$\hat{l}_z = -1 \qquad \hat{s}_z = -\frac{w}{3+h}. \tag{19}$$

At $h = 0$ this transforms to the result obtained in [11]. At $h = 0$ this mode is stable in the region

$$0 < \hat{s}_z < \frac{\sqrt{41}-1}{10}. \tag{20}$$

In table 1 equation (19) is compared with the results of computer simulation.

All of the above-listed six states were reproduced, stabilized and identified with a computer simulation program developed by Leman and Golo [5]. In this program the Leggett equations are numerically solved in the presence of finite dissipation, which is compensated by the power supply from the RF field. The numerical results for stable RO and RS–TS states are discussed in the appendix. We used large dissipation to decrease the computing time; nevertheless the results agree within a few per cent with those obtained above in the mean-field approximation, i.e. when $\Omega_L^2 \ll \omega_L^2$, and in the limit of no dissipation and power absorption. Equation (14), which goes beyond the mean-field theory, was also reproduced in numerical simulations.

At different phases of the Larmor precession, the precessing states can form spatial domains in the experimental cell, separated from each other by phase boundaries. Until now only one such interface, that separating HPD and NPD, has been observed and exploited [1]. One may expect other interfaces to exist. In particular, the interface between RS–TS and RO domains can be stabilized by an applied magnetic field gradient. Since the RS–TS domain exists at a positive frequency shift and the RO domain exists at a negative frequency shift, the position r of this phase boundary is defined by the same equation, $\gamma H(r) = \omega$, as the position of the interface between HPD and NPD.

The way that new states have been obtained in numerical simulation can give us some hint on how to reach these states in real NMR experiments. In particular, a simple way to obtain the RS–TS and RO modes is to push the HPD mode to its RS edge, $\hat{s}_z = -1$ (see figure 2), where the HPD becomes unstable towards a reorientation of the $\hat{l}$ vector from the parallel to the transverse direction. The thus-formed RS state then relaxes to the RS–TS state if the applied frequency shift is positive, $w > 0$, or to RO at negative frequency shift, $w < 0$. At large negative frequency shift the RO mode appears to be unstable towards the formation of the KV state with a non-equilibrium magnitude of spin: $|S| = \frac{1}{2}\chi H$. In another scenario the RS mode with $\hat{s}_z = -1$, $\hat{l}_z = 0$ continuously passes along the vertical line of figure 1 with a decrease in the magnitude of the magnetization until it reaches one half of the equilibrium magnetization, and then relaxes to one of the KV states.

Among all the precessing states the BS and HPD modes have the lowest dissipation; that is why only the HPD mode has been exploited at moderate temperatures. The reason is that both the BS mode and the HPD mode, when close to $\hat{s}_z = -1/4$, correspond to the true minimum of the dipole energy and therefore the dipole torque is nearly absent for these states, which means a negligibly small Leggett–Takagi relaxation. The other states correspond to the minimum of the dipole energy averaged over the period of precession. This means that the instantaneous dipole torque is non-zero, and therefore the Leggett–Takagi relaxation is essential for these states. The other modes should be observed at lower temperature where dissipation decreases. It is not clear, however, if the new modes are related to the new NMR regime found at low temperature [4].

Acknowledgments

This work has been supported through the ROTA co-operation project between the Academy of Finland and the Russian Academy of Sciences. I am grateful to Yu M Bunkov, V L Golo, G A Kharadze, J S Korhonen, and M Krusius for fruitful

discussions. I am indebted to Yu M Bunkov, G R Pickett and G A Kharadze for providing me with their manuscripts prior to publication, to V L Golo and A A Leman for kind permission to use their computer program to solve the Leggett equations, and to A V Babkin for kind permission to use his computer terminal.

Appendix

We have used a computer program developed by Leman [5] to solve numerically the Leggett equations:

$$\partial_t \boldsymbol{S} - \boldsymbol{H} \times \boldsymbol{S} = \boldsymbol{T} \tag{A1}$$

$$\partial_t \boldsymbol{R}_i = \boldsymbol{R}_i \times \left(\boldsymbol{H} - \frac{\boldsymbol{S} + \tau \boldsymbol{T}}{\chi} \right). \tag{A2}$$

Here the dipole torque is

$$\boldsymbol{T} = -\boldsymbol{R}_i \times \frac{\delta F_D}{\delta \boldsymbol{R}_i} \tag{A3}$$

and the dipole energy

$$F_D(\boldsymbol{R}_i) = F_D(R_{\alpha i}) = \tfrac{2}{15} \chi \Omega_L^2 (\mathrm{Tr}\ \mathbf{R} - \tfrac{1}{2})^2. \tag{A4}$$

The external field $\boldsymbol{H}$ consists of the constant field $\boldsymbol{H}_0$ and the transverse RF field $\boldsymbol{H}_{RF}(\omega) \perp \boldsymbol{H}_0$ with the frequency ω close to the Larmor frequency $\omega_L = H_0$. We have used $H_0 = 330$ G and $\Omega_L = 250$ kHz; all other parameters are given in the table. We maintained a continuous linearly polarized RF field, H_{RF}, which corresponds to $H_{RF}/2$ for the proper circularly polarized component, i.e. for the component that precesses in the same direction as the magnetization. The pumping from the RF field compensates the energy losses, caused by dissipation, according to the following equation:

$$\omega H_{RF} S_\perp \sin \alpha = \tau T^2 \tag{A5}$$

where α is the angle between the precessing RF field and the precessing transverse magnetization. In the table the dissipation is described by the parameter of longitudinal relaxation, $\Gamma = \tau \Omega_L^2$.

The analytical values of $\hat{s}_z$ were calculated using (19) for the RO mode, which exists at negative frequency shifts $w < 0$, and (17) for the RS–TS mode, which exists at positive frequency shifts $w > 0$. The values for w and h were obtained using (7); it is important that in the equation for h one should use half of the magnitude of the RF field, since only one circularly polarized component of the field is important.

References

[1] Borovik-Romanov A, Bunkov Yu, Dmitriev V V and Mukharsky Yu 1984 *Pis. Zh. Eksp. Teor. Fiz.* **40** 256 (Engl. Transl. 1984 *JETP Lett.* **40** 1033)
Fomin I A 1984 *Pis. Zh. Eksp. Teor. Fiz.* **40** 260 (Engl. Transl. 1984 *JETP Lett.* **40** 1037)

[2] Kondo Y, Korhonen J S, Krusius M, Dmitriev V V, Mukharsky Yu M, Sonin E B and Volovik G E 1991 *Phys. Rev. Lett.* **67** 81

[3] Kondo Y, Korhonen J S, Krusius M, Dmitriev V V, Thuneberg E V and Volovik G E 1992 *Phys. Rev. Lett.* **68** 3331

[4] Bunkov Yu M, Fisher S N, Guenault A M and Pickett G R 1992 *Phys. Rev. Lett.* **69** 3092

[5] Golo V L and Leman A A 1991 *Physica* B **169** 525
Golo V L and Leman A A 1990 *J. Low Temp. Phys.* **80** 89

[6] Kharadze G and Vachnadze G 1992 *Pis. Zh. Eksp. Teor. Fiz.* **56** 474 (Engl. Transl. 1992 *JETP Lett.* **56** 458)

[7] Misirpashaev T Sh and Volovik G E 1992 *Zh. Eksp. Teor. Fiz.* **101** 1197 (Engl. Transl. 1992 *Sov. Phys.–JETP* **75** 650)

[8] Fomin I A 1978 *J. Low Temp. Phys.* **31** 509

[9] Abragam A and Goldman M 1982 *Nuclear Magnetism: Order and Disorder* (Oxford: Clarendon)

[10] Korhonen J S, Dmitriev V V, Krusius M, Parts Ü, Bunkov Yu M, Kondo Y, Mukharskiy Yu M and Thuneberg E V 1992 *Report TKK-F-A702* Otaniemi, Finland (1993 *Phys. Rev.* B submitted)
Bunkov Yu M and Timofeevskaya O 191 *Pis. Zh. Eksp. Teor. Fiz.* **54** 232 (Engl. Transl. 1991 *JETP Lett.* **54** 228)

[11] Korhonen J S and Volovik G E 1992 *Pis. Zh. Eksp. Teor. Fiz.* **55** 358 (Engl. Transl. 1992 *JETP Lett.* **55** 362)

[12] Fomin I A 1990 *Modern Problems in Condensed Matter Sciences 26: Helium Three* ed W P Halperin and L P Pitaevskii (Amsterdam: North-Holland) p 610